# Leaky Lamb waves in an anisotropic plate. II: Nondestructive evaluation of matrix cracks in fiber-reinforced composites

Vinay Dayal, and Vikram K. Kinra

Citation: The Journal of the Acoustical Society of America **89**, 1590 (1991);
View online: https://doi.org/10.1121/1.401017
View Table of Contents: http://asa.scitation.org/toc/jas/89/4
Published by the Acoustical Society of America

# Leaky Lamb waves in an anisotropic plate. II: Nondestructive evaluation of matrix cracks in fiber-reinforced composites

Vinay Dayal
*Department of Aerospace Engineering and Center for Non-Destructive Evaluation, Iowa State University, Ames, Iowa 50011*

Vikram K. Kinra
*Mechanics and Materials Center and Aerospace Engineering Dept., Texas A&M University, College Station, Texas 77843*

(Received 20 March 1989; accepted for publication 24 November 1990)

This paper is concerned with the use of leaky Lamb waves for the nondestructive evaluation (NDE) of damage in anisotropic materials such as fiber-reinforced composites. Two fundamental acoustic properties of the material, namely, the wave speed and attenuation have been measured. Stiffness is deduced from the wave speed. The damage mode selected for this study is matrix cracking. As expected, the in-plane stiffness decreases and the attenuation increases with an increase in the linear crack density.

PACS numbers: 43.20.Fn, 43.40.Le

## INTRODUCTION

Matrix cracking, generally, is the first mode of failure in fiber-reinforced composites. This is a micro-level failure and not being self-sustaining mechanism, is distributed throughout the structure. By self-sustaining is meant here that, once a crack has developed, it may not propagate any further upon subsequent loading. The reason for this behavior is that the strong fibers act as crack arresters and stress relieving takes place in the vicinity of the cracks. As a result, stresses are again distributed all over the structure and further cracking takes place elsewhere. These cracks are called matrix cracks. Though the integrity of the structure is not lost due to the matrix cracks, overall stiffness of the structure is reduced, and its damping is increased.

Composites are being used as load bearing members, especially in the aerospace structures, because of their excellent strength-to-weight ratio and the designer's ability to tailor the directional properties to the service requirements. Reduction in stiffness, due to damage, can result in change in response of the structure upon loading. This change is important for the designer as well as the user. Ultrasonic techniques such as "*C* scan" have been used to detect larger defects, but evaluation of residual stiffness is still an ongoing problem. Hence, a nondestructive evaluation of the composite structure is necessary where even before large size defects can be monitored, changes in stiffness should be measured.

Ultrasonic NDE has been used for the through-the-thickness evaluation of cross-ply fiber-reinforced composites.[1-3] It was found that although the ultrasonic attenuation was a very sensitive damage metric, wave speed was not. Thus attenuation measurement can be used to estimate damage in composites. Master curves[3] of attenuation as a function of crack length show such a possibility of NDE application. The reason for this behavior becomes clear from Fig. 1(a). In the through-the-thickness mode, the wave travels normal to the plate and the cracks also lie in the same plane. Obviously, the wave–crack interaction is minimal. As mentioned earlier, although changes in attenuation are measured, the wave speed, or stiffness, is not affected. Moreover, out-of-plane stiffness is not of much use to the designer, while in-plane stiffness is an important design criteria. The in-plane reduction in stiffness of cross-ply laminates has been modeled by a number of researchers. Highsmith and Reifsnider[4] have used the shear lag model theory to estimate the reduction in Young's modulus of cross-ply laminates. Talreja[5] has measured the initial and final stiffness values in the composites and predicts the intermediate values by using a continuum damage model. Hashin[6] has analyzed $[0^\circ_m/90_n]_s$ type laminates by variational methods on the basis of the principle of minimum complementary energy. This gives a lower bound for the reduction in stiffness. He has analyzed the laminates for both Young's modulus and

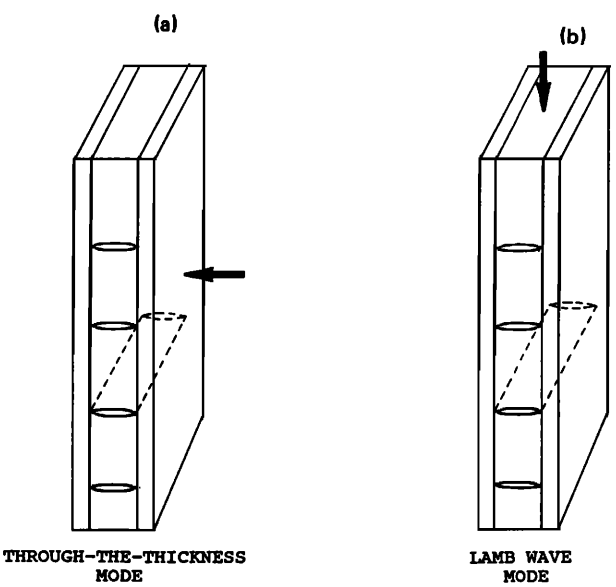


FIG. 1. Wave propagation direction, shown by arrows, with respect to transverse cracks in a cross-ply laminate.

 0001-4966/91/041590-09$00.80  

shear modulus reductions. Laws and Dvorak[7] have based their model on the fracture mechanics concepts and incorporate $G_{IC}$ of the material in the model. Also, since all the advanced composites are processed at an elevated temperature and then cooled down to room temperature, the model incorporates the residual stresses in the laminate. Allen *et al.*[8] has modeled the stiffness reduction using internal state variables (ISV) and has analyzed the curved cracks to estimate the stiffness reduction. Almost all models assume that the cracks are normal to loading direction while it is observed that with many cracks, especially when the number of cracks becomes large, the cracks are curved or angled; hence, their model is noteworthy. Bai Jia-Min[9] has used the integral equation approach to model the stiffness reduction in cross-ply laminates. This is not an attempt to list all models in this area of research. Interested readers can refer to Laws and Dvorak[7] for a more comprehensive list.

Experimentally, the stiffness reduction has been measured by the stress–strain curve. Highsmith and Reifsnider[4] and Allen *et al.*[8] have measured the stiffness reduction by plotting the stress–strain curves. To avoid any further damage while the stress–strain curve is drawn, the loads are kept very low so that no further damage is induced. This can also be achieved by using the unloading part of the curve. This type of experimental work is ideal if the material follows the Kaiser law. According to this, the damage cannot increase if the load applied is less than the load which produced the damage in the first place. It is observed that in composites much smaller load than the damage inducing load can add to the existing damage state. Also, these techniques are not nondestructive and though they have applications in a laboratory setting are not applicable in in-field testing. A nondestructive method such as ultrasonic technique will be more suitable for tests on actual structure. Hence, we have attempted to use ultrasound for measurement of stiffness reduction. The in-plane stiffness can be measured very conveniently by waves traveling in the plane of the plate. This mode of wave propagation is called the Lamb wave (or plate wave) mode. In this mode the waves travel in the plane of the plate or normal to the cracks, see Fig. 1(b), and hence the crack–wave interaction will be large and it is expected that wavespeed will be sensitive to the changes in in-plane stiffness.

When the plate is immersed in a fluid, the Lamb waves traveling in the plate leak energy into the surrounding fluid as shown in Fig. 2. These waves in the fluid have been named "Leaky Lamb waves." These leaky Lamb waves can be sensed by a transducer and the wave speed and attenuation in the plate material can be measured. It may be noted here that in the Lamb wave mode of wave propagation, attenuation in undamaged specimens is due to: (1) energy leaked into the fluid, and (2) the material nonuniformity as a result of the damage. We assume that the attenuation due to leakage remains essentially constant but the attenuation due to damage increases with damage. Hence, the measured increase in attenuation is attributed to the induced damage. The Lamb wave speed, on the other hand, is related to the overall stiffness in the plane of the plate and hence the changes in wave speed are due to the change in the in-plane

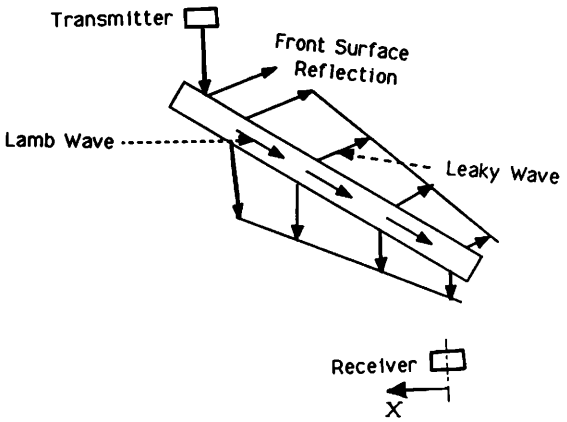


FIG. 2. Generation and propagation of Lamb waves in a plate immersed in water.

stiffness as the damage increases. A continuum damage state is assumed due to large wavelength of the ultrasound used in the tests.

Bar-Cohen and Chementi[10] have utilized the leaky Lamb waves for the nondestructive testing (NDT) of damage in fiber-reinforced composites. They have shown that various forms of damage can be identified by a null-zone movement method. When a wave is incident upon the plate, a specular reflection from the plate front surface takes place along with the generation of Lamb waves in the plate. Due to phase change in the leaky waves, the specular reflection and the leaky wave interfere and a well-defined null zone is observed; the movement of this null zone has been related to various defects. A *C*-scan type setup was used to map the damage. Lamb waves have been used by Tang and Henneke[11] for the measurement of stiffness reduction in laminated composites. They have used a method similar to acousto-ultrasonic experiments. By proper frequency tuning they achieve the lowest antisymmetric mode wave to travel in the plate and measure the wave speed changes. Our studies show that in the basic antisymmetric mode the reduction in wave speed is predominantly due to the reduction in shear stiffness and is least sensitive to the changes in axial stiffness.

In this work we have utilized the leaky Lamb waves for the NDE of composites. The receiving transducer is placed in such a position that the specular reflection is completely avoided and only the leaky waves are sensed. Shown in Fig. 2 is the relative position of the transmitter and the receiver. For reasons detailed later, we use the basic symmetric mode in our work. The wave speed and attenuation in the specimen are measured from the received signal. The specimen is damaged and transverse cracks are introduced in the cross-ply laminates. Changes in wave speed and attenuation are measured to estimate the damage. We present here some results for the NDE of cross-ply laminates by leaky Lamb waves. It is observed that attenuation increases and in-plane stiffness decreases as damage is induced in the composites. The technique has a good potential for field application since it is nondestructive and is the only NDE technique available for the in-plane stiffness measurement. Furthermore, as will be shown later, it yields *local* values of properties.

## I. THEORY

The detailed derivation of the dispersion equations for a general balanced symmetrical composite laminate immersed in a fluid is reported in a companion paper.[12] In this work the composite is modeled as a homogeneous anisotropic material. Other models that take into consideration the microstructure are listed in Ref. 12. The basic symmetrical mode ($s_0$) has been selected for the tests. The reason for this selection will be described in details in the results section. It will suffice to mention at this stage that in this mode the wave travels as a plane-fronted wave. Also, the wavelength of the wave is large in comparison to the crack-size and therefore the composite can be treated as an anisotropic homogeneous material. In this mode it has been shown[13] that, when $fd$ is small, then

$$c^2 = E_1/\rho(1 - \nu_{12}\nu_{21}), \tag{1}$$

where $f$ is the test frequency, $2d$ is the plate thickness, $c$ is the Lamb wave speed, $E_1$ is an in-plane modulus, and $\nu_{12}$ and $\nu_{21}$ are the two in-plane Poisson's ratios. For the composites tested during this investigation $\nu_{12}\nu_{21} \ll 1$ and hence Eq. (1) reduces to

$$c^2 = E_1/\rho. \tag{2}$$

The refraction of ultrasonic waves through a plate follows the Snell's law of refraction:

$$\sin(\theta_i)/\sin(\theta_r) = v_\omega/c, \tag{3}$$

where $v_\omega$ is the wave speed in water, $\theta_i$ and $\theta_r = \pi/2$ are the angles of incidence and refraction, respectively. Thus

$$c = v_\omega/\sin(\theta_i) \tag{4}$$

combining Eq. (4) with Eq. (2),

$$E_1 = \rho[v_\omega/\sin(\theta_i)]^2. \tag{5}$$

This equation is used for the measurement of the in-plane stiffness in this work.

It is obvious from Eq. (5) that the measurement of $\theta_i$ will be an important factor in the accuracy of measurement. A very simple but elegant method has been devised to accurately ascertain the Lamb angle. As shown in Fig. 2 the receiver is moved by a distance $x$. A very elementary calculation (see the Appendix) shows that at the correct Lamb angle, total travel time from the emitter to the receiver is independent of $x$. Thus, though the receiver is moved on its traveling mechanism, the signal on the oscilloscope remains unchanged on the time scale; only its amplitude is reduced. It was determined that the Lamb angle could be measured with a precision of 0.1 deg, which was also the accuracy of our instrumentation. The decrease in the amplitude of the signal as the receiver is moved, is recorded and by fitting an exponential curve through the points, the attenuation coefficient is calculated. Thus, in one experiment, the attenuation is obtained and the validity of the Lamb angle is also checked. The accuracy of measurement of modulus is estimated to be 2%, and for attenuation it is about 10%.

## II. EXPERIMENTAL PROCEDURE

The block diagram of the experimental setup is shown in Fig. 3. The pulse generator produces a trigger signal which is used to trigger the signal generator and also to set the initial time for the digitizing oscilloscope. The pulse generator produces a train of sinusoidal signal. Since these signals are typically of a few volts in amplitude, a power amplifier is used to amplify the signal to about 200 V. This amplified signal is then fed into the transmitting transducer. The transducer produces an ultrasonic wave which is transmitted through the water and specimen to the receiving transducer. The receiver sends the signal to the signal amplifier, which provides the oscilloscope with a signal of about 1 V. The digitizing oscilloscope averages the signal over 64 samples and stores the average. On demand from the computer, the necessary information is provided by the oscilloscope over an IEEE-488 bus. The wave speed and attenuation are then calculated. Entire operation of the oscilloscope is controlled by the computer.

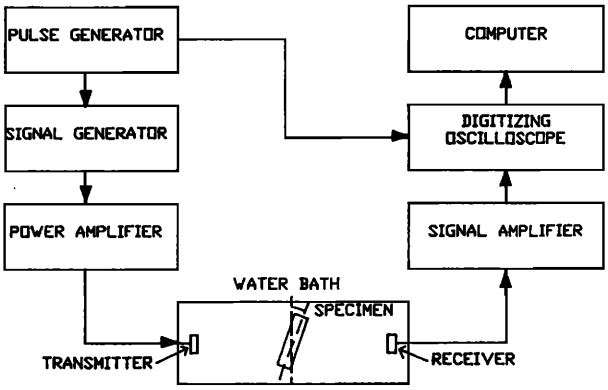


FIG. 3. Block diagram of the experimental setup.

Water is used as an acoustic couplant; the transducers are mounted inside a water bath. Transmitter and receiver are mounted on two traveling mechanisms graduated to 0.001 in and the specimen is placed in a holder mounted on a turntable which is graduated to 0.1 deg. When the specimen is rotated to achieve the correct Lamb angle, the length of the specimen between the transducer is increased. To offset this increase, the two transducers are moved laterally such that same length of the specimen is interrogated throughout the experiments. Since repeatability is very important in our measurements, the specimen holder is designed so that exact replacement of the specimen is achieved every time. The specimen is carefully placed against a tab fixed on the specimen holder on each replacement. A typical plot of received signal, as the specimen is rotated, is given in Fig. 4.

All composite specimens are made of Magnamite *AS*4/3502 graphite/epoxy prepreg tapes manufactured by Hercules Inc. Transverse cracks were chosen to be the mode of damage for all the studies reported here. Toward this end, cross-ply laminates with layups of the type $[0_m/90_n]_s$ were fabricated. Typically, the specimens are plates of $1 \times 11$-in. size.

All loading, to induce damage in the specimen, was performed on INSTRON model 125 equipped with a 20 000 pound load cell. The tests were conducted in the stroke-control mode. The cross-head speed used was 0.05 in./min in the

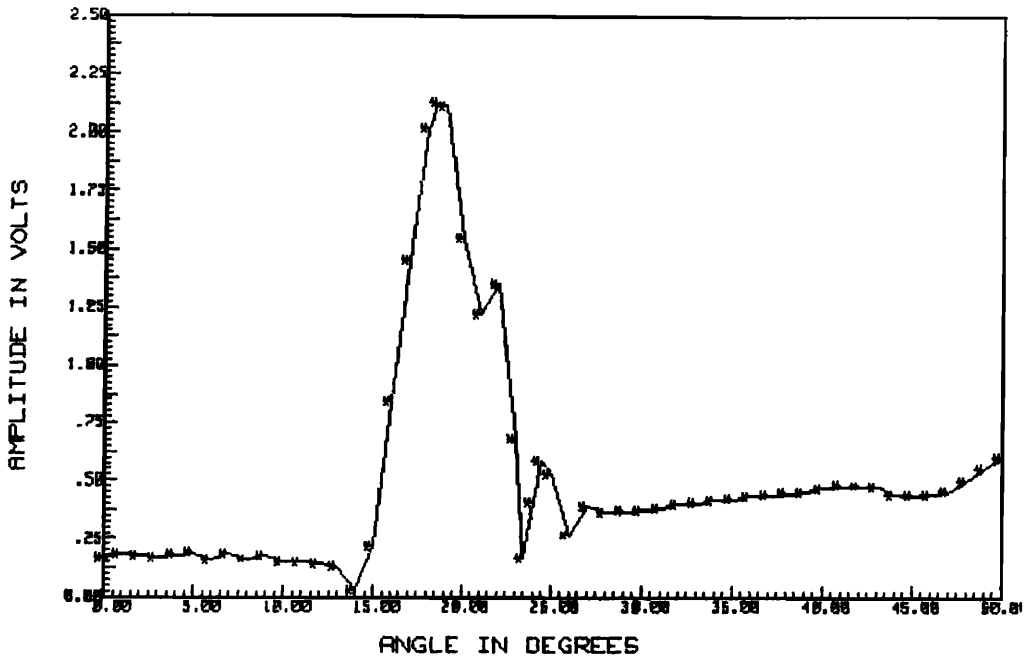


FIG. 4. Angle of incidence versus the received signal amplitude.

initial stages of damage. When nearing the ultimate strength of the specimen the speed was reduced to 0.02 in./min.

The edges of the specimens were polished with 5- and 1-$\mu$m alumina powder. This is done to get good quality edge replications. A record of the cracks developed in the specimen was maintained in the form of edge replications. In order to open the cracks, the specimens are loaded in the INSTRON machine to about 500 pounds. The replicating tape is softened by acetone and pressed against the edge of the specimen. The softened tape material flows into the crack and hardens in about 30 s. The tape is removed and the replica of the cracks can be viewed under a microfiche reader.

In the early stages of this work, water seepage into the cracks was found to be a major source of error and this was prevented by coating the edges with a strippable coat (mfg. Sherwin Williams).

## III. RESULTS AND DISCUSSIONS

Dispersion equations for Lamb waves in isotropic materials are available in the published literature; they were solved[14] based on the assumption that the attenuation due to leakage is negligibly small. This assumption is reasonably valid as long as $\rho^1/\rho \gg 1$, where $\rho^1$ and $\rho$ are the densities of the plate and the immersion fluid, respectively. If one is studying the steel/water system, then $\rho^1/\rho$ is, in fact, large compared to 1. However, for the fiber-reinforced composites studied in this work, $\rho^1/\rho = 1.53$ and therefore, neglecting the inertial loading of water will result in gross error in the dispersion curves as also shown by Plona *et al.*[15] Therefore, we have derived an exact solution for the dispersion equations for an anisotropic plate immersed in a fluid and have obtained the dispersion curves as well as the attenuation curves. These have been reported in an earlier paper.[12] (Some results from the work are reproduced in Fig. 7 for the sake of continuity.) In this work the nonhomogeneous anisotropic plate is replaced by a homogeneous anisotropic plate and the dispersion relations are derived. Thus the microstructure of the composite plate is not taken into consideration. This theory should break down when $fd$ becomes large. We have tested this laminate up to an $fd = 1.6$ and at this $fd$ the wave speed for the $s_0$ mode is 2 mm/$\mu$s. For a plate thickness of 0.49 mm, the wavelength $\lambda = 0.61$ mm. This shows that our model behaves well even when the wavelength is on the order of a characteristic length, the half-plate thickness. Even for $s_2$ mode, where $\lambda = 2.1$ mm, the model does not break down. Despite this, we have restricted our tests to much lower values of $fd$, due to reasons listed below.

Before embarking on the NDE of composites, we performed some numerical calculations to study the sensitivity of various wave speeds and frequencies on different components of the stiffness matrix. The four elastic constants $c_{11}$, $c_{33}$, $c_{55}$, and $c_{13}$ are the contributors to the dispersion equations. There is no simple method to predict the relation between the change in Lamb wave speed and the degradation of one of these stiffness constants. In isotropic plates there are some well-established conjectures because the relations are simple, but when the dispersive equation is complicated and four stiffness coefficients appear, we have performed this sensitivity analysis. In this study, one stiffness coefficient is decreased at a time and the corresponding Lamb wave speed calculated. The studies are made on a $[0/90_4]_s$ laminate. The effects of the degradation in stiffness constants on the basic symmetric and asymmetric modes, $s_0$ and $a_0$, respectively, are studied. The results for the symmetric mode at an $fd = 0.25$ MHz mm ($kd = 0.32$; here $k = 2\pi f/c$ is the wave number) are shown in Fig. 5(a). Quite expectedly, only $c_{11}$ contributes significantly to the reduction in the wave speed. The effect of $c_{33}$ and $c_{13}$ is very small and the effect of $c_{55}$ is practically zero. An interesting result is that, if the degradation takes place in $c_{13}$, then the wave speed increases; the effect is, however, very small. Shown in Fig.

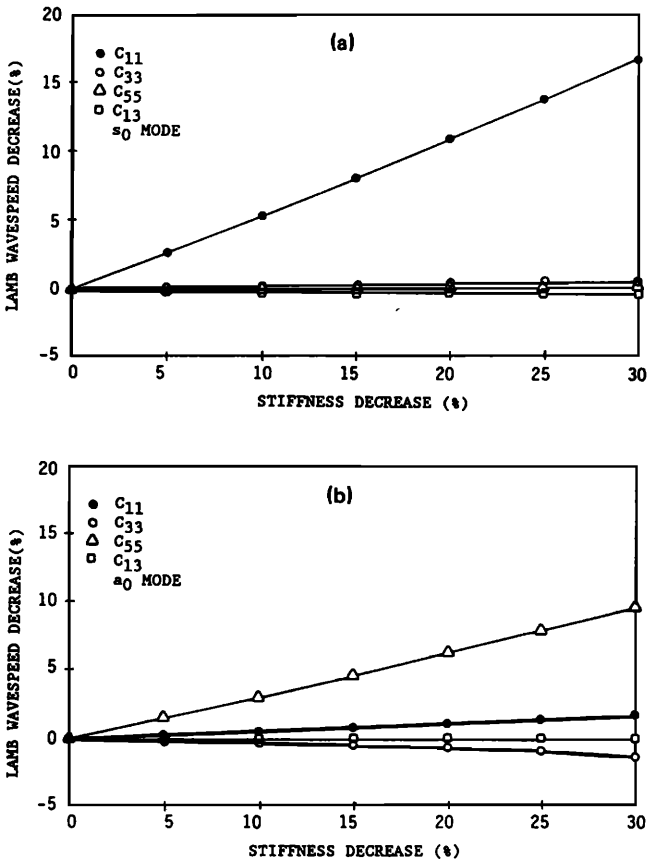


FIG. 5. Effect of degradation in stiffness coefficients in a $[0/90_4]_s$ laminate on Lamb wave wave speed of (a) $s_0$ mode and (b) $a_0$ mode.

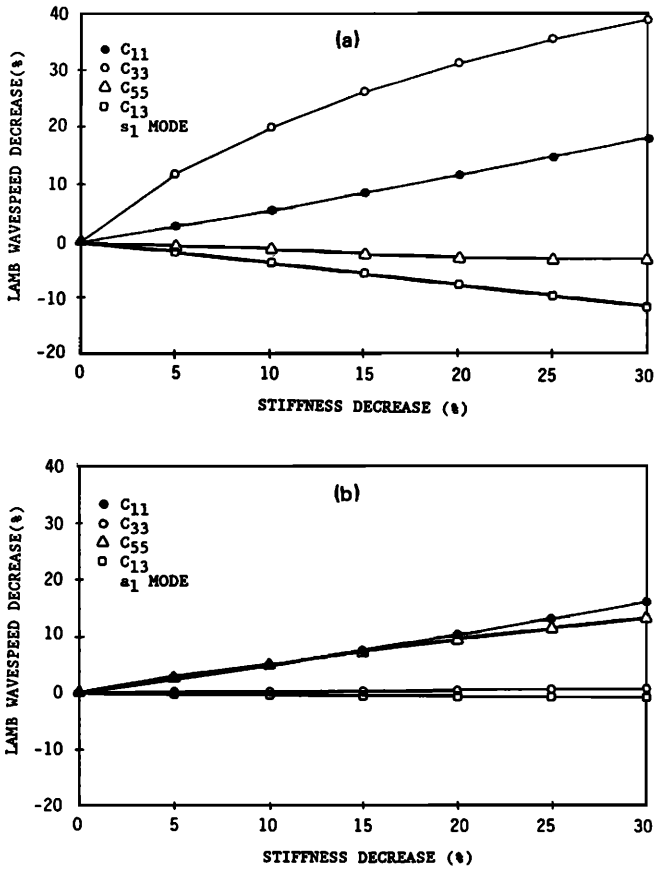


FIG. 6. Effect of degradation in stiffness coefficients in a $[0/90_4]_s$ laminate on Lamb wave wave speed of (a) $s_1$ mode and (b) $a_1$ mode.

5(b) is the effect of stiffness degradation on the $a_0$ mode at $fd = 0.5$ MHz mm ($kd = 0.63$). Now, $a_0$ is the fundamental flexural mode and is well known that shear deformation plays a significant role in the propagation of flexural waves. Accordingly, it is observed that the major contributor in this case is $c_{55}$, but contributions due to $c_{11}$ and $c_{33}$ are not negligible. A decrease in $c_{33}$ results in an increase in Lamb wave speed. However, $c_{13}$ does not contribute to the change in wave speed.

The results for the next higher modes, $s_1$ and $a_1$, are shown in Fig. 6. The effect of $s_1$ mode is studied at $fd = 2.00$ MHz mm ($kd = 2.53$). For this mode the major contribution comes from the $c_{33}$ and $c_{11}$. On the other hand, degradation in $c_{55}$ and $c_{13}$ will tend to increase the wave speed and their contributions are not negligible. The results for $a_1$ mode are at $fd = 0.6$ MHz mm ($kd = 0.76$). Here, the degradation in $c_{11}$ and $c_{55}$ effect in the same order and $c_{33}$ and $c_{13}$ effects are negligible.

The conclusions of this study are that the Lamb wave technique is useful in measuring the degradation in $c_{11}$, which can be done with tests conducted in $s_0$ mode. To some extent, by using the $a_0$ mode the degradation in $c_{55}$ can be studied. Since contributions from other modes will also affect the Lamb wave speed, the measurements will not be reliable for the case of $a_0$ mode. A combination of tests may prove to be useful. For example, the degradation in $c_{33}$ and $c_{11}$ can be measured by tests in $s_1$ mode. If the ratio of these degradations is estimated, then the effect of $c_{33}$ can be separated. Similarly, the effect of $c_{55}$ can be measured by combining $a_1$ and $s_0$ modes. Based on this sensitivity study, it was decided to carry out all measurements in the $s_0$ mode.

First, the tests were performed on a $[0/90_3]_s$ graphite/epoxy composite laminate. The dispersion curves for this specimen are shown in Fig. 7(a). The solid lines are for symmetric mode and dashed lines for asymmetric modes. The attenuation curves for various modes are shown in Fig. 7(b). The tests for Lamb wave speed and attenuation in undamaged specimens, as described earlier, are performed and the results are shown as discrete points on Fig. 7. The theoretical curves are from stiffness values calculated by the rule of mixtures;[16] the agreement between theory and experiments is considered satisfactory. The static stiffness of the laminate was also measured in a tensile testing machine and the corresponding wave speed is shown as an arrow in Fig. 7(a). This shows that, if the experimentally determined values of the stiffness constant are used in the dispersion relations, then a better correlation between the theory and experiments will be observed. It is observed from Fig. 7(b) that the attenuation of the $s_0$ mode remains very small up to an $fd = 0.5$ MHz mm and then increases very sharply. This attenuation is due to energy leaked into the water. This is another reason why we have chosen to perform our tests in the low $fd$ values. When the attenuation is very high, the reception and identification of waves will become difficult as

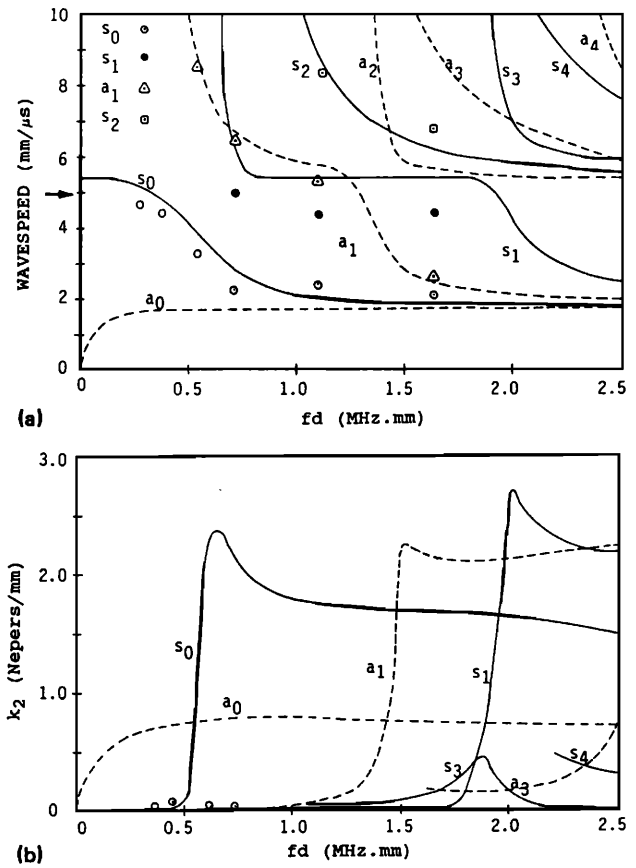


FIG. 7. Dispersion and attenuation curves for $[0/90_4]_s$ laminate. The circled data are experimental.

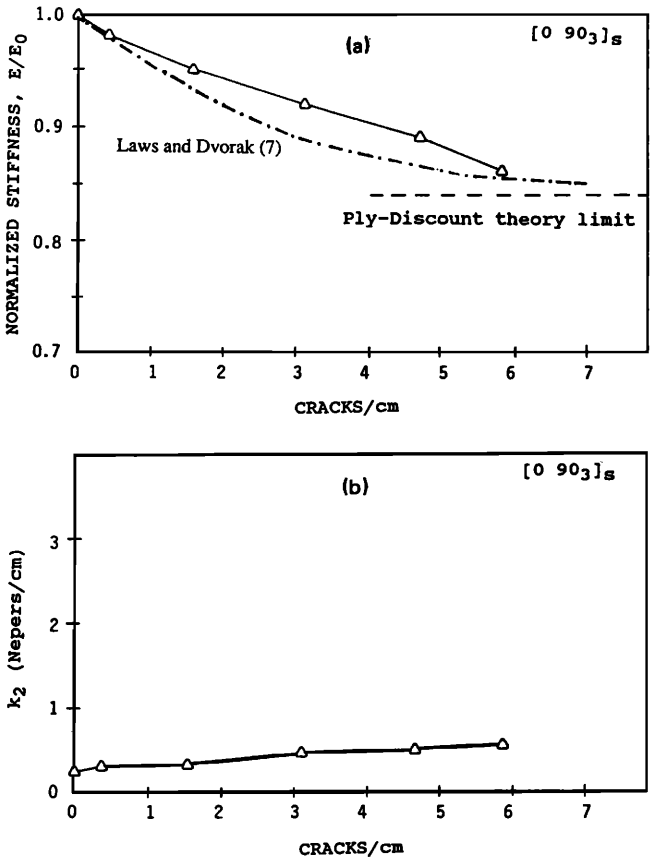


FIG. 8. (a) Reduction in stiffness, and (b) increase in attenuation of $[0/90_3]_s$ laminate, $f = 0.5$ MHz, $d = 0.55$ mm.

they will decay very rapidly. Also, the changes in attenuation due to microcracks cannot be measured reasonably if they ride over a very high attenuation value.

Now, the same $[0/90_3]_s$ laminate is tested to study the effect of transverse cracks on the Lamb wave speed and attenuation. The tests are conducted at a frequency of 0.5 MHz with $fd = 0.275$ MHz mm ($kd = 0.34$). The reduction in the normalized stiffness as a function of number of cracks per centimeter, as damage progresses, is shown in Fig. 8. The normalized stiffness is defined as $E/E_0$, where $E_0$ is the stiffness of the undamaged laminate and $E$ is the stiffness of the damaged laminate. The figure also shows a dashed horizontal line which denotes the stiffness of the damaged laminate calculated by the ply-discount theory (Ref. 16, Chap. 6). In this theory the stiffness of the cracked lamina is assumed to be zero in the direction normal to the crack and the laminate stiffness is synthesized. The experimental results obtained by the Lamb wave technique are within the lower limit set by the theoretically obtained limit. Shown also is the curve obtained by using the theory developed by Laws and Dvorak,[7] and a fair comparison between theory and experiments is observed.

Next, a $[0/90_4]_s$ laminate is tested when damage is induced in it. The test is performed at 0.5 MHz with $fd = 0.355$ MHz mm ($kd = 0.44$). The reduction in stiffness for this laminate is shown in Fig. 9. Also shown in the figure is the damage state and the position of the transmitter (TR) and receiver (R) relative to the specimen. It is observed that, in going from damage state 3 to state 4, though there was a substantial increase in the total number of cracks in the specimen, the number of cracks in the region interrogated by the transducer did not increase. As a consequence, no change in the stiffness of the specimen was recorded. This is very reassuring for it demonstrates that our measurement reflects local changes in the stiffness. For this specimen, stiffness reduced by about 30% as compared to the virgin state. The dashed line shows the stiffness reduction as calculated from the ply-discount theory but for this specimen the measured stiffness was slightly lower than the theoretically calculated value. The curve obtained by using the Laws and Dvorak theory[7] is also plotted. We see a reasonable correlation in the beginning, but later the theory predicts a lower stiffness reduction. This can be explained by the fact that the theory assumes that the cracks are all straight and parallel, while the edge replications show that many cracks are formed at an angle or they are straight in the middle of the 90° ply group, but, as they approach the 0° interface, the cracks turn sharply. Hence, the surface energy requirements in the two cases will be different. In comparison to the reduction for the $[0/90_3]_s$ laminate, it is observed that the stiffness reduction for this laminate is larger. The reason for this is that the net contribution of the eight-90° plies to the overall stiffness is more than the contribution of six-90° plies and hence failure of plies in the $[0/90_4]_s$ laminates results in a

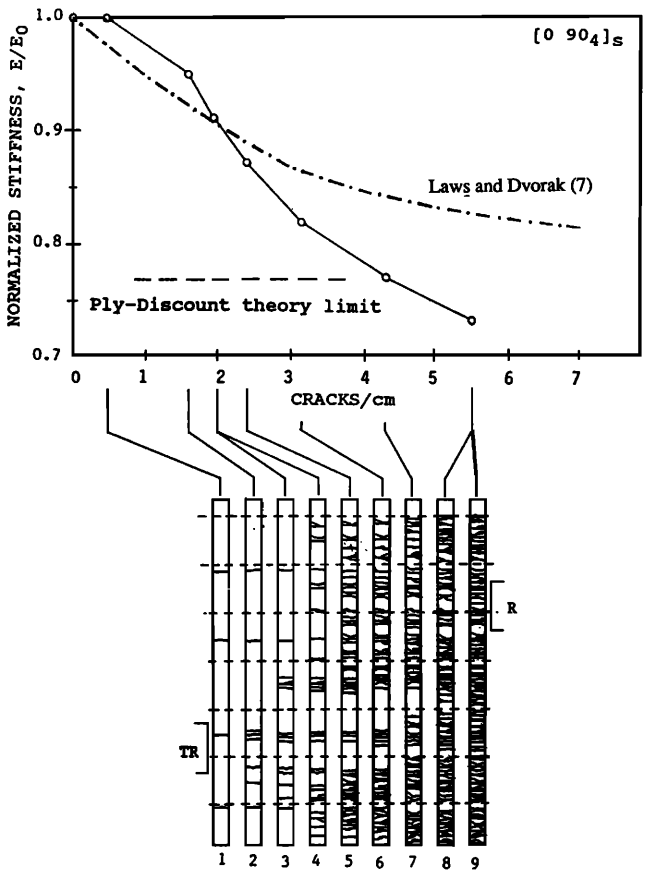


FIG. 9. Reduction in stiffness as transverse cracks increase in a $[0/90_4]_s$ laminate, $f = 0.5$ MHz, $d = 0.71$ mm. Line sketch shows damage state.

higher reduction in relative stiffness. Observe that the $[0/90_3]_s$ laminate has a crack length of 6-ply thickness long while the $[0/90_4]_s$ laminate has a larger crack length of 8-ply thickness long.

The next set of tests were performed on a $[0_2/90_2/0]_s$ laminate. For this laminate the crack size is very small, namely, 2-ply-thickness long. The reduction in stiffness as transverse cracks are introduced is shown in Fig. 10. Observe a smaller reduction in stiffness. Even though this laminate has four-90° plies, they are divided into groups of two, and also, the total number of 0° plies in this laminate is increased three times. Thus the total contribution of the 90° plies to the overall stiffness is very low and hence their failure results in less reduction in stiffness.

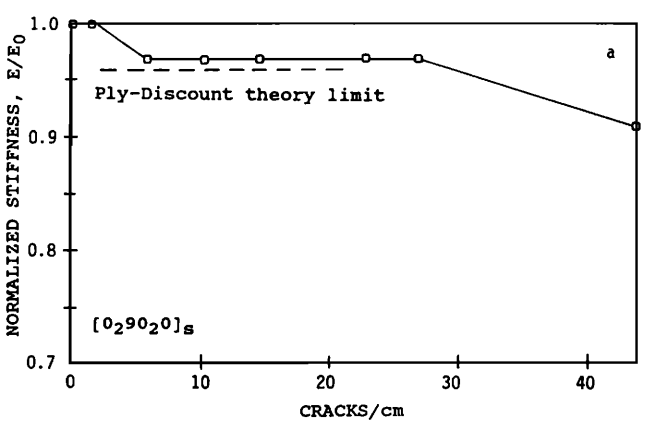


FIG. 10. Reduction in stiffness in a $[0_2/90_2/0]_s$ laminate, $f = 0.5$ MHz, $d = 0.71$ mm.

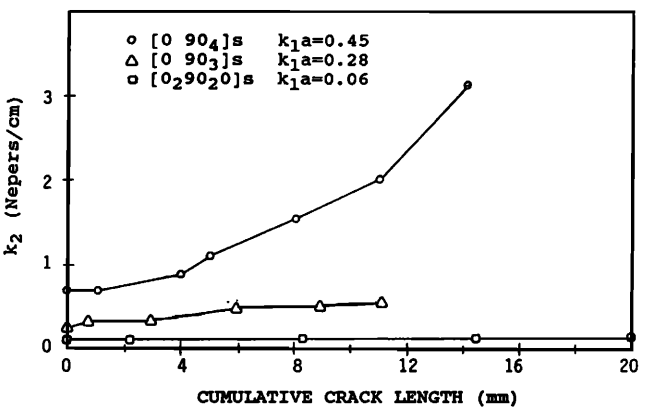


FIG. 11. Relative study of the increase in attenuation for the three laminates tested.

The attenuation increase in the three laminates tested are combined together and shown in Fig. 11. Shown also in the figure are the $k_1 a$ values for the three laminates Here, $k_1$ is the wave number of the Lamb wave, $2a$ is the crack length which is equal to the thickness of 90° ply group in the laminate, and $k_2$ is the attenuation in Nepers/cm. The purpose behind this presentation is to demonstrate the effect of the normalized scattering cross section of the cracks, $k_1 a$, on the attenuation. In this context we cite an excellent work by Tan[17] who has calculated the normalized scattering cross section of a Griffith crack subjected to a longitudinal plane wave loading; see Fig. 12. Since Tan's calculation is for an unbounded medium, it cannot be applied quantitatively to the present case. However, it does provide an excellent background in which the present results can be explained qualitatively. In $[0_2/90_2/0]_s$ laminate $k_1 a = 0.06$. As is well known, this is the so-called Rayleigh scattering regime where the scattering cross section of a crack is very small. The waves pass through the plate without seeing the cracks and as a result the increase in attenuation is very low. For

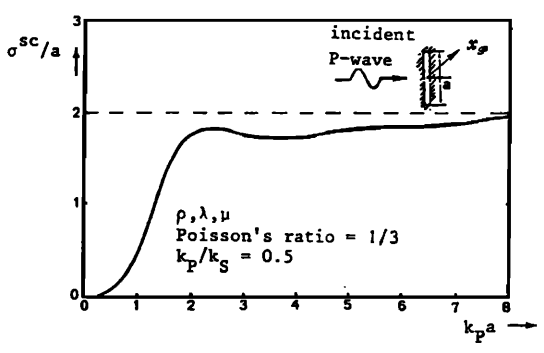


FIG. 12. Normalized plane-wave extinction cross-section for the scattering of a $P$ wave by a crack of finite width. [Ref. (17) reprinted by permission of Kluwer Academic Publishers].

$[0/90_3]_s$ laminate $k_1 a = 0.26$, while for the $[0/90_4]_s$ laminate $k_1 a = 0.45$ and the observed increase in attenuation is very high. The effect of $k_1 a$ on measured attenuation is very interesting. Kinra[18] has worked with composites consisting of lead spheres in an epoxy matrix and has shown that the wave propagation in these composites occurs along two separate branches: (1) the low-frequency, slower, acoustical branch along which the particle motion is essentially in phase with the excitation, and (2) the high-frequency, faster, optical branch along which the particle displacement is essentially out of phase of the excitation. The two are separated by a cutoff frequency which corresponds to the excitation of the rigid-body-translation resonance of the heavy inclusion. This occurs when $k_1 a = 0(1)$, where $a$ is the inclusion radius. Around the cutoff frequency, both the phase velocity, as well as the attenuation, change very dramatically. This phenomenon is shown in Fig. 13 taken from our earlier work.[19] Based on the results it can be said that a similar phenomenon is taking place in these laminates and the cracks act as inclusions.

These results forewarn against an arbitrary selection of the test frequencies. Depending on the flaw size, $a$, the test frequency, and hence the $k_1 a$, has to be chosen such that a good signal amplitude decay curve is obtained. If the attenuation falls very slowly with damage then it will not be a sensitive measure of the damage. On the other hand if the attenuation falls very rapidly then at a relatively low crack density the received signal will be lost and the measurement will be inaccurate.

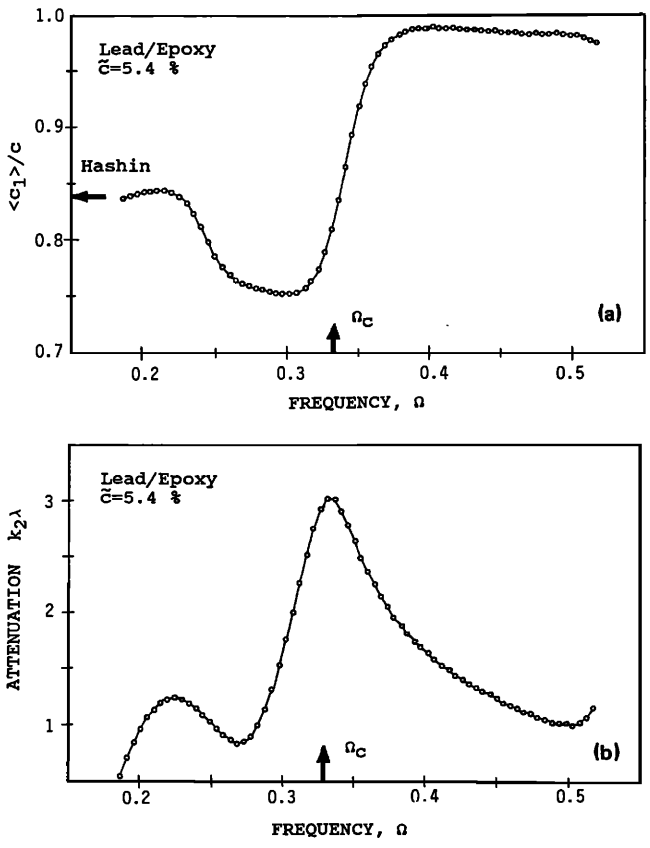


FIG. 13. (a) Normalized phase velocity and, (b) attenuation variation with normalized frequency, $\Omega(\Omega = k_1 a$, where $a$ is inclusion radius), in lead–epoxy composite at volume fraction $c$ (Ref. 12).

## IV. CONCLUSIONS

Propagation of a leaky Lamb wave in its fundamental mode in three cross-ply laminates: $[0_2/90_2/0]_s$, $[0/90_3]_s$, and $[0/90_4]_s$ have been studied experimentally. The effect of matrix cracking on the speed (i.e., stiffness) and attenuation was studied in the long wavelength regime. As expected, it was found that the in-plane stiffness *decreases* while the attenuation *increases* with linear crack density. Therefore, either of these quantities may be used to measure the damage-induced degradation of the in-plane stiffness. A particular advantage of this method is that one can measure the local values (average over the transducer diameter) of stiffness. The attenuation, on the other hand, is averaged over the distance that the receiver moves.

## ACKNOWLEDGMENTS

This research was supported by the Air Force Office of Scientific Research under Grant No. *AFOSR*-84-0066 to Texas A&M University. The program managers were Dr. David Glasgow and Dr. George Haritos.

## APPENDIX

The schematic of the signal traveling through the specimen is shown in Fig. A1. When the receiver is at its initial location $i$, the total travel time from the transmitter to receiver is

$$t_i = \frac{l_1}{c_w} + \frac{l_2}{c} + \frac{l_4}{c_w}, \qquad \text{(a)}$$

where $c_w$ is the wave speed in water and $c$ in the specimen.

As the receiver is moved by a distance $x$ to $f$, the travel time becomes

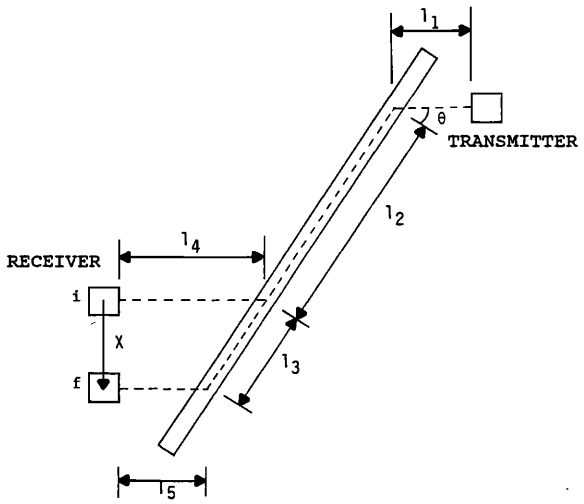


FIG. A1. Travel time for a Lamb wave in a plate.

$$t_f = \frac{l_1}{c_w} + \frac{l_2}{c} + \frac{l_3}{c} + \frac{l_5}{c_w}. \quad \text{(b)}$$

The difference in the two arrival times is

$$\Delta t = t_f - t_i = \frac{l_3}{c} + \frac{l_4 - l_5}{c_w} = \frac{l_3}{c} - \frac{x\tan(\theta)}{c_w}$$

$$= \frac{x}{c\cos(\theta)} - \frac{x\tan(\theta)}{c_w}. \quad \text{(c)}$$

Substituting Snell's Law Eq. (4) into $c$

$$\Delta t = [x/c\cos(\theta)] - [x\tan(\theta)/c\sin(\theta)] = 0.$$

This shows that at the correct Lamb angle, when the receiver is moved by an arbitrary distance, the total time taken by the wave to travel from the emitter to receiver remains unchanged.


[1] H. I. Ringermacher, "Ultrasonic Velocity Characterization of Fatigue Damage in Graphite/Epoxy Composites," Proc. IEEE 1980 Ultrasonic Symp., Boston, 957–960 (1980).

[2] J. H. Cantrell, Jr., W. P. Winfree, J. H. Heyman, and J. D. Whitcomb, "Multiparameter Characterization of Fatigue Damage in Graphite/Epoxy Composite Material," Proc. IEEE 1980 Ultrasonic Symp., Boston, 1003–1005 (1980).

[3] J. G. Eden, "The Application of Ultrasonics to Assess Damage in Composite Materials," M.S. thesis, Texas A&M University, College Station, TX 77843 (1985).

[4] A. L. Highsmith and K. L. Reifsnider, "Stiffness-reduction Mechanisms in Composite Laminates," in *Damage in Composite Materials*, ASTM STP 775, 103–117 (1982).

[5] R. Talreja, "Transverse Cracking and Stiffness Reduction in Composite Laminates," J. Compos. Mater. **19**, 355–375 (1985).

[6] Z. Hashin, "Analysis of Stiffness Reduction of Cracked Cross-Ply Laminates," Eng. Fracture Mech. **25** (5/6), 771–778 (1986).

[7] N. Laws and G. J. Dvorak, "Progressive Transverse Cracking in Composite Laminates," J. Compos. Mater. **22**, 900–916 (1988).

[8] D. H. Allen, C. E. Harris, S. E. Groves, and R. G. Norvell, "Characterization of Stiffness Loss in Cross-ply Laminates with Curved Matrix Cracks," J. Compos. Mater. **22**, 71–81 (1988).

[9] Bai Jia-Min, "Stiffness Reduction Analysis of Cracked Cross-ply Laminates by Using Integral Equation Approach," Eng. Fracture Mech. **34** (1), 245–251 (1989).

[10] Y. Bar-Cohen, D. E. Chementi, "NDE of Defects in Composites Using Leaky Lamb Waves," Proc. of 15th Symp. on NDE Sponsored by NTIAC & SWRI and South Texas Section of ASNT, San Antonio, TX (1985).

[11] B. Tang and E. G. Hennekke II, "Lamb-wave Monitoring of Axial-Stiffness Reduction of Laminated Composite Plates," Mater. Eval. **47**, 928–934.

[12] V. Dayal and V. K. Kinra, "Leaky Lamb Waves in an Isotropic Plate.I–An Exact Solution and Experiments," J. Acoust. Soc. Am. **85**, 2268–2276 (1989).

[13] C. C. Habegar, R. W. Mann, and G. A. Baum, "Ultrasonic Plate Waves in Paper," Ultrasonics, 57–62 (1979).

[14] L. G. Merkulov, "Damping of Normal Modes in a Plate Immersed in a Liquid," Sov. Phys. Acoust. **10** (2) (1964).

[15] T. J. Plona, M. Baharavesh, and W. G. Mayers, "Rayleigh and Lamb Waves at Liquid Solid Boundaries," Ultrasonics, 171–174 (1975).

[16] B. D. Agarwal and L. J. Broutman, *Analysis and Performance of Fiber Composites* (Wiley, New York, 1980).

[17] T. H. Tan, "Scattering of Plane Elastic Waves by a Plane Crack of Finite Width," J. Appl. Sci. Res. **33**, 75–100 (1977).

[18] V. K. Kinra, "Dispersive Wave Propagation in Random Particulate Composites," in *Recent Advances in Composites in the United States and Japan*, edited by J. R. Vinson and M. Taya, ASTM STP 864, pp. 309–325 (1985).

[19] V. K. Kinra and V. Dayal, "A New Technique for Ultrasonic Nondestructive Evaluation of Thin Specimens," Exp. Mech. **28** (3), 288–297 (1988).